Structure and function of human muscle fibres and muscle proteome in physically active older men

Lorenza Brocca*[1,2] Jamie S McPhee[7], Emanuela Longa[1], Monica Canepari[1,2], Olivier Seynnes[5], Giuseppe De Vito[6], Maria Antonietta Pellegrino[1,2,3], Marco Narici[8] and Roberto Bottinelli[1,3,4]

*corresponding author

[1]Department of Molecular Medicine, University of Pavia, Pavia, Italy

[2]Interuniversity Institute of Myology, University of Pavia, Pavia, Italy

[3]Interdipartimental Centre for Biology and Sport Medicine, University of Pavia, Pavia, Italy

[4]Fondazione Salvatore Maugeri (IRCCS), Scientific Institute of Pavia, Pavia, Italy

[5]Department of Physical Performance, Norwegian School of Sport Sciences, Oslo, Norway.

[6]Institute for Sport and Health, University College Dublin, Ireland

[7]School of Healthcare Science, Manchester Metropolitan University, Manchester, United Kingdom

[8]School of Graduate Entry to Medicine and Health, Division of Clinical Physiology, University of Nottingham, Derby, UK

The authors declare no conflict of interest.

* To whom correspondence may be addressed at: Department of Molecular Medicine, via Forlanini 6, 27100 Pavia. E-mail: lorenza.brocca@unipv.it

key words: aging, single fibres, specific force, proteome

Key points

• Loss of muscle mass and strength in the growing population of elderly people is a major health concern for modern societies. This condition, termed sarcopenia, is a major cause of falls and of the subsequent increase in morbidity and mortality

• Despite numerous studies on the impact of ageing on individual muscle fibres, the contribution of single muscle fibres adaptations to ageing induced atrophy and functional impairment is still unsettled

• The level of physical function and disuse is often associated with aging

• We studied relatively healthy older adults in order to understand the effects of aging per se without the confounding impact of impaired physical functional

• We found that in healthy ageing structural and functional alterations of muscle fibres occur. Protein post-translational modifications, oxidation and phosphorylation, contribute to such alterations more than loss of myosin and other muscle proteins content

Abstract

Contradictory results have been reported on the impact of ageing on structure and functions of skeletal muscle fibres likely due to complex interplay between ageing and other phenomena such as disuse and diseases. Here we recruited healthy, physically and socially active young (YO) and elderly (EL) men in order to study aging *per se* without the confounding effects of impaired physical function. I*n vivo* analyses of quadriceps and *in vitro* analyses of vastus lateralis muscle biopsies were performed. In EL subjects, our results show that: (i) quadriceps volume, maximum voluntary torque (MVC), and patellar tendon force (Ft) were significantly lower; (ii) muscle fibres went through significant atrophy and impairment of specific force (Po/CSA) and unloaded shortening velocity (Vo); (iii) myosin/actin ratio and myosin content in individual muscle fibres were not altered; (iv) muscle proteome went through quantitative adaptations, namely an up-regulation of the content of several groups of proteins among which myofibrillar proteins and antioxidant defence systems; (v) muscle proteome went through qualitative adaptations, namely phosphorylation of several proteins, including Myosin Light Chain-2 slow and Troponin T and carbonylation of Myosin Heavy Chains. The present results indicate that impairment of individual muscle fibres structure and function is a major feature of ageing *per se* and that qualitative adaptations of muscle proteome are likely more involved than quantitative adaptations in determining such phenomenon.

Abbreviations

ACTA, actin; ACTC, actin α cardiac; ALDOA, fructose-biphosphate Aldolase A; BAP, brightness–area product; CAH3, Carbonic anhydrase III; COX5A, Cytochrome c oxidase sub 5A; CRYAB, α-β-crystallin; CSA, cross-sectional area; DLDH, Dihydrolipoyl dehydrogenase; EL, elderly; GSTM2, GAPDH, Glyceraldehyde 3-P dehydrogenase; Glutathione-S-transferase Mu; GSTP1, Glutathione -*S*-transferase P; HBA, Hemoglobin sub alpha; HBB, Hemoglobin sub beta; HSPB6, Heat Shock Protein beta 6; LDHA, lactate dehydrogenase; MB, myoglobin; MHC, myosin heavy chain; MLC, myosin light chain; P_0, isometric force; P_0/CSA, specific force; PEBP1, Neuropolypeptide h3; PGM1, Phosphoglucomutase; PKM, pyruvate kinase; PRDX2, Peroxiredoxin 2; PRDX3, Peroxiredoxin3; PRDX6, Peroxiredoxin6; PSMA2, Proteasome α-sub isoform 2; ROS, reactive oxygen species; SOD1, Cu/Zn Superoxide dismutase; TNNT1, troponin T slow; TNNT3, troponin T fast; TPM1, tropomyosin alpha chain; UQCRC1, Ubiquinol-cytochrome c reductase; UQCRC2, Cytochrome b-c1 complex sub2; V_0, unloaded shortening velocity; YO, young.

Introduction

Loss of muscle mass and strength in the growing population of elderly people is a major health concern for modern societies. This condition, generally termed sarcopenia (Evans & Campbell, 1993; Fielding *et al.*, 2011), is a major cause of falls and of increased in morbidity and mortality in older people.

Multiple phenomena occurring at molecular, cellular and whole muscle levels can cause sarcopenia. Interestingly, as a disproportionate loss of muscle force compared to muscle mass has been observed (Servais *et al.*, 2007) it has been understood that ageing can cause changes in muscle "quality" and not only in muscle "quantity". Several qualitative adaptations can affect, at variable extents, muscle function (Narici & Maffulli, 2010): increased fat and connective tissue content, variations in muscle architecture and tendon compliance, neuromuscular junction integrity and excitation-contraction coupling, changes in muscle fibres type distribution and contractile properties. Moreover, analysis of muscle proteome has shown post-translational modifications (Baraibar *et al.*, 2013; Li *et al.*, 2015) and changes in content of muscle proteins (Gelfi *et al.*, 2006; Capitanio *et al.*, 2009) independently from a change in total protein content.

Single muscle fibre structure and function are major determinants of muscle size and of the intrinsic capacity to develop force of whole muscles in vivo. The impact of ageing on individual muscle fibres has been extensively studied. Contradictory results have been reported and the contribution of single muscle fibres adaptations to ageing induced atrophy and functional impairment is still unsettled. Consistent with some earlier work (Larsson *et al.*, 1997; D'Antona *et al.*, 2003), muscle fibre atrophy and impairment in muscle fibre specific force and unloaded shortening velocity have been considered major factors causing sarcopenia. However, others reported no atrophy and no impairment of specific force and of shortening velocity in elderly compared to young men and women (Trappe *et al.*, 2003). It has been suggested that discrepancies could be due to the different habitual physical activity background of the populations studied (D'Antona *et al.*, 2007). Indeed, exercise training can improve muscle fibre function (Trappe *et al.*, 2000; D'Antona *et al.*, 2006), whereas disuse, which frequently occurs with ageing, is known to cause atrophy and impairment of muscle fibre function (Brocca *et al.*, 2015). Consistently, a study reported no difference in cross sectional area (CSA), specific force and unloaded shortening velocity of individual muscle fibres from young and elderly individuals matched for physical activity levels (Hvid *et al.*, 2011). These observations clearly indicate that habitual physical activity levels can modulate muscle fibre ageing, but one cannot ignore the fundamental finding that muscle mass, strength and power decline with ageing even in master athletes (Shanely *et al.*, 2002; Shanely *et al.*, 2004).

Not surprisingly, the causes of the loss of muscle fibre intrinsic function (force per unit area and unloaded shortening velocity) in ageing are still unsettled. In sedentary and immobilized elderly subjects, lower specific force of muscle fibres has been attributed to lower myosin concentration (D'Antona *et al.*, 2003). Post-translational modifications have been shown to occur in ageing and potentially affect the capacity of myosin to develop force and shortening (Li *et al.*, 2015). Ageing has been suggested to cause alterations in myosin structure and in acto-myosin interaction possibly due to myosin oxidation (Prochniewicz *et al.*, 2007). Moreover, recent proteomic analyses have shown that in ageing, alterations can occur not only in myosin content, but in the content of many myofibrillar proteins and of other functional groups of proteins (e.g. metabolic enzymes and anti-oxidant defence systems) (Gelfi *et al.*, 2006; Capitanio *et al.*, 2009). The latter observations underlie the complexity of the adaptations in muscle protein pattern and suggest factors in addition to myosin can impair muscle fibre function. However, it is difficult to unequivocally attribute the above potential causes of muscle fibre function impairment to ageing, as reduced physical activity has confounding effects. In healthy young adults, disuse has been shown to cause lower specific force of muscle fibres based on lower myosin concentration (Borina *et al.*, 2010; Brocca *et al.*, 2015). Moreover, protein oxidation (Dalla Libera *et al.*, 2005) and myosin light chain phosphorylation (Maffei *et al.*, 2014) have been shown to occur in disuse and potentially affect myosin function (Coirault *et al.*, 2007; Maffei *et al.*, 2014). Finally, disuse can cause profound alterations in muscle proteome, which partially overlap with those observed in ageing (Brocca *et al.*, 2012; Brocca *et al.*, 2015; Hvid *et al.*, 2016).

The aim of the present study was to examine the structure and function of single muscle fibres and to identify underlying causes of functional impairments affecting fibres of older people. To reduce the

confounding impact of disuse and diseases on ageing, we recruited relatively healthy, physically and socially active older and younger men according to procedures previously described (McPhee *et al.*, 2013a). As impairment of muscle fibre function could depend on adaptations of muscle protein content we studied myosin concentration and myosin/actin ratio in single muscle fibres and assessed adaptations in whole protein pattern by proteome analysis (2-DE) of bulk muscle samples. The potential role of qualitative adaptations of proteins, namely oxidation and phosphorylation, was assessed by oxy-blot of myosin heavy chains and of muscle proteins and by phosphoproteome analysis of proteome 2-DE gels.

The present work suggests that structural and functional alterations of muscle fibres occur as part of the normal ageing process. Post-translational modifications, namely oxidation and phosphorylation, of several muscle proteins contribute to such alterations more than loss of myosin and other muscle proteins content.

Methods

Subjects and muscle biopsies

Ten elderly subjects (EL age 70.9 ± 4.1 years) and 10 young control subjects (YO age 23.0 ± 2.2 years) were enrolled in the study. All subjects received and signed the informed consent. The study conformed to the principles of the Declaration of Helsinki on human experimentation and was approved by the ethics committee from Manchester Metropolitan University Both populations were physically active and free from any musculoskeletal or chronic disease known to impact on physical activity levels. As reported by McPhee et al. (McPhee *et al.*, 2013a), physically active subjects were defined as "those involved in moderate or vigorous activities where the intention was to improve health and fitness. Activity sessions should work up a sweat and last around 30 min per session, for around 3 sessions per week and individuals must have consistently maintained such activities for the majority of the year and for the past 3 years or more". The older participants completed the Voorrips physical activity questionnaire (score 8.5 ± 0.9), assessment of grip strength (37.4 ± 2.2 kg) and walking speed during the 6 min walk test (1.64 ± 0.06 m/s) as previously described (McPhee *et al.*, 2013b) to confirm they were not sedentary nor likely to be sarcopenic or frail based on commonly used screening assessments (Cruz-Jentoft *et al.*, 2010). Those involved in competitive exercise were excluded.

Muscle samples were taken by needle biopsy under local anesthesia from the vastus lateralis muscle using a procedure previously described (Bergstrom, 1979; Bottinelli *et al.*, 1996). Muscle samples were divided in several portions: two were immediately frozen in liquid nitrogen and used for myosin heavy chain (MHC) and myosin light chain (MLC) isoform distribution analysis, myosin/actin ratio analysis, MLC phosphorylation analysis, proteomic analysis, phosphoprotein analysis and protein oxidation analysis. One piece of biopsy was divided in smaller bundles, stored at -20°C in skinning solution (150 mm potassium propionate, 5 mm KH_2PO4, 5 mm magnesium acetate, 3 mm Na_2ATP, 5 mm EGTA, pCa 9.0) plus 50% glycerol and used to determine the cross-section area (CSA), force (P_o), maximum shortening velocity (V_o) and myosin concentration of dissected single fibers.

In vivo analyses

Magnetic resonance imaging

The right knee and thigh was imaged using a 0.25-T MRI scanner (G-scan, Esaote Biomedica, Genoa, Italy) as participants lay supine with both legs fully extended (Shoepe *et al.*, 2003). Transverse-plane cross sections were collected from the tibial tubercle of the knee joint through to the anterior-inferior iliac spine of the hip using Turbo-3D T-1 weighted protocols and 2.8 mm thick slices with 0 mm distance between slices. Using off-line computer software (OiyriX, Pixmeo, Switzerland), anatomical cross-sectional area of the quadriceps muscles was measured at 25mm intervals from distal to proximal ends of the quadriceps and integrated to estimate quadriceps muscle volume (Qvol) (Shoepe *et al.*, 2003). A sagittal-plane scan of the entire knee joint was also collected using the same scanning parameters. From the centre image, the mid-point between the surface of the femoral condyles and the tibial plateau was located and a measurement taken as a straight line from this point to intercept perpendicular with the mid-point of the patella tendon to estimate patella tendon moment arm length (Shoepe *et al.*, 2003). The moment arm values were multiplied by 0.99 to account for the fact that the images were collected with a fully extended knee joint, but isometric torque was measured at 90° knee flexion (Song *et al.*, 2009).

Patella tendon force

Knee extension maximal voluntary contraction isometric torque (MVC) was assessed at 90° knee angle (where full knee extension is 0°) with the back supported at 85° (where lying supine is 0°) and a strap firmly securing the hips to the dynamometer chair and the ankle to the lever arm 2 cm above the ankle malleolus. A familiarisation and warm-up included 3 - 5 contractions at around 50% of maximal effort each lasting around 3 s and another two further contractions at around 80% maximal effort. After a short rest, participants performed a maximal effort by increasing torque voluntarily and sustaining the maximal effort for around 3 s. Visual feedback was available to the participants and verbal encouragement was provided. The highest of three maximal efforts was taken as MVC.

The patella tendon force (Ft) was estimated by dividing the MVC by the patella tendon moment arm length. The quadriceps in vivo specific force was estimated by dividing the Ft by quadriceps muscle volume.

Single fiber analysis

Cross-sectional area (CSA), force and maximum shortening velocity of single muscle fibres were analyzed as previously described in detail (Bottinelli et al. 1994, 1996). Briefly, segments of single fibres were manually isolated from muscle bundles with the help of a stereomicroscope at 20-40X magnifications in a muscle chamber containing skinning solution (K-p 150 mM, KH2PO4 5mM, MgAc 5 mM, DTT 1 mM, EGTA 5 mM, Na2-ATP 3 mM, pH 7, Leupeptine Hydrochloride 20µg/ml, E64 10 µM). The fibres were immersed for 1 h in skinning solution containing 0.1% Triton X-100 and afterward returned to the previous skinning solution. Each fibre was mounted between two hooks on a stage of an inverted microscope; CSA and length (2-3 mm) were measured in order to calculate the volume assuming an elliptical shape of the cross section. The width and the depth of the fibres were measured with an inverted microscope at 320x magnification on 10 different positions along the fiber. Using the mean values of width and the depth, CSA was determined. The volume was then calculated by multiplying CSA and length thus obtained.

Isometric force (P_0) and unloaded shortening velocity (V_0) were measured by the slack test technique. Briefly, each fibre was placed in activation solution: 100 mm KCl, 20 mm imidazole, 5 mm MgCl2, 5 mm Na2ATP, 0.5 mm EGTA, 25 mm creatine phosphate, 300 U ml^{-1} creatine kinase, pCa 8.0. Experiments were performed at 12°C, in conditions of maximal activation (pCa 4.5) and at optimal sarcomere length (2.5 µm) for force developing (Bottinelli & Reggiani, 2000; D'Antona et al., 2003). For each of the 10 elderly and young subjects, at least 10 single muscle fibres were dissected. At the end of mechanical experiment, fibres were characterized on the basis of MHC isoform composition. Assuming that there are no variations between subjects, a general average of all single muscle fibre value was made for each functional parameters analysed.

Myosin concentration analysis

Myosin concentration analysis was performed using an approach previously described in detail (D'Antona et al., 2003; Borina et al., 2010) with some modifications. After mechanical experiments, the fibres were placed in 30 µl of standard buffer (Soriano et al., 2006) at 4 °C for 18 h to complete myosin extraction. Subsequently, 10 µl and 20 µl of buffer in which the fibre segment was dissolved, were loaded on 12% linear polyacrylamide gel, run at 16 mA for 4 h at 4 °C and stained with Colloidal Coomassie (Gelcode Blue Stain Reagent – Pierce). In the same gel, a known amount of myosin standard were loaded in order to determine a standard curve.

The brightness–area product (BAP) of the myosin bands was determined on gels imaged using the software Adobe Photoshop CS3 (Adobe). BAP correspond to product of the number of pixels of the whole MHC band for the mean intensity level of the pixels. The myosin concentration standard curve was built plotting together BAP values from myosin standard and known amount of myosin loaded. Finally, BAP values evaluated for each single fiber were inserted in the standard curve obtaining their myosin concentration.

Myosin/actin ratio analysis

Muscle biopsies, previously stored at −80°C, were pulverized with liquid nitrogen and immediately suspended in lysis buffer (50 mM Tris-HCl pH 7.6, 250 mM NaCl, 5mM EDTA, 1.5% v/v β-mercaptoethanol and 2% inhibitor-proteases cocktail by Sygma-Aldrich). A protein assay kit (RC DC Biorad) was used to determine protein concentration. For each subject 10 μg of sample were loaded into a precast gradient gel (AnykD, Biorad). The gel run 1 h at room temperature at 100 V and then it was stained with Coomassie Blue and acquired with a high resolution scanner (EPSON expression 1680 Pro). The brightness–area product (BAP) of myosin and actin bands of each sample was measured using the software Adobe Photoshop CS3 (Adobe) and the myosin-actin ratio was then calculated.

Myosin heavy chain isoform distribution analysis

Separation and identification of myosin heavy chain (MHC) isoforms in single fibres and in whole biopsy was performed as previously described (Bottinelli *et al.*, 1996; D'Antona *et al.*, 2003; Pellegrino *et al.*, 2011a). Single muscle fibre segments used for mechanical experiments were dissolved in Laemmli solution (Soriano *et al.*, 2006) and loaded on 6% SDS-PAGE polyacrylamide gels. Electrophoresis was run overnight at 100 V; following silver stain, three bands were separated in the region of MHC isoforms.

MHC isoform composition was assessed in the whole biopsy. In this case, frozen portion of biopsy was pulverized in a steel mortar with liquid nitrogen to obtain a powder that was immediately resuspended in a in Laemmli solution (Soriano *et al.*, 2006). The samples were incubated in ice for 20 min and finally spun at 18000 g for 30 min. Protein concentration in the dissolved samples was determined with a protein assay kit (RC DC Biorad). About 10 μg of proteins for each sample were loaded on 6% SDS-PAGE polyacrylamide gels and the electrophoresis was run overnight at 100 V; following Coomassie stain, three bands corresponding to MHC isoforms were separated and their densitometric analysis was performed to assess the relative proportion of MHC isoforms (MHC-1, MHC-2A and MHC-2X) in the samples (Pellegrino *et al.*, 2003; Pellegrino *et al.*, 2011a).

Proteome analysis (2-DE)

Sample preparation.

Muscle samples, were prepared with the same procedures used previously (Brocca et al., 2010). Frozen portion of biopsy was pulverized in a steel mortar with liquid nitrogen to obtain a powder that was immediately resuspended in a lysis buffer (8 M urea, 2 M thiourea, 4% Chaps, 65mM DTT and 40 mM Tris base). The samples were vortexed, frozen with liquid nitrogen, thawed at room temperature four times, incubated with DNase and RNase for 45min at 4∘C to separate proteins from nucleic acids and finally spun at 18000 g for 30 min. Protein concentration in the dissolved samples was determined with a protein assay kit (2D quant Kit, GE Healthcare). A sample mix was obtained for each experimental group (YO and EL). Sample mix contained an equal protein quantity taken from each muscle sample of young and elderly subjects.

Two-dimensional electrophoresis.

First dimension, isoelectrofocusing, was carried out using IPGphor system (Ettan IPGphor isoelectric Focusing Sistem - GE Healthcare). 150 μg of proteins were loaded on IPG gel strips, pH 3-11 NL (non linear) 13 cm, that were rehydrated for 14h, at 30 Volt and at 20°C, in 250 μl of reswelling buffer (8 M urea, 2 M thiourea, 2% (w/v) CHAPS, 0.1% (v/v) tergitol NP7 (Sigma), 65 mM DTT, 0.5% (v/v) pharmalyte 3-11NL (GE Healthcare)). Strips were focused at 20000 Vhr, at constant temperature of 20°C and limiting the current to 50 μA per IPG gel strip. After isoelectrofocusing the strips were stored at -80°C until use or equilibrated immediately for 10-12 min in 5 ml of equilibration buffer (50 mM Tris pH 6.8, 6 M urea, 30% (v/v) glycerol, 2% (w/v) SDS, 3% (w/v) iodoacetamide). Then, the immobiline IPG gel strips were applied to 15% T, 2.5% C polyacrylamide gels without a stacking gel. The separation was performed at 80 V for 17h at room temperature.

2D gels were fixed for 2h in fixing solution (ethanol 40% (v/v) acetic acid 10% (v/v)), stained with fluorescent staining (FlamingoTM Fluorescent Gel Stain by BIO-RAD) for 3h and destained with 0.1% (w/v) Tween 20 solution for 10 minutes.

Triplicate gels of each sample group were obtained, visualised using a Typhoon laser scanner (GE Healthcare) and analysed with Platinum Software (GE Healthcare). For the analysis, we have chosen one gel as a master gel to perform automatic spots matching. Only the spots present in all gels were considered for analysis. The variation of the expression of each spot was evaluated by calculating the ratio between the average volume of a given protein expressed in the EL group and the average volume of the same spot in the YO group. In the x-axis of the histogram, positive numbers indicate upregulation whereas negative numbers downregulation of the spots. 2D gels were used to find the protein differences. All spots statistically changed ($P < 0.05$) were considered and then analysed by Mass Spectrometry in order to identify the corresponding protein.

Phosphoproteome analysis

For this analysis the same samples prepared for proteome analysis were used. Before electrophoretic run, the samples were delipidated and desalted in order to obtain an adequate separation and subsequent staining specific for phosphoproteins. 600 µl of methanol, 150 µl of chloroform and 450 µl of ultrapure water were added at 150 µl of samples (300 µg of proteins) and the samples were centrifuged at 18000 g for 5 minutes. After discarding the upper phases, 450 µl of methanol were added and the samples were spun at 18000 g for 5 minutes. Finally, the pellet was resuspended in reswelling buffer (8 M urea, 2 M thiourea, 2% (w/v) CHAPS, 0.1% (v/v) tergitol NP7 (Sigma), 65 mM DTT, 0.5% (v/v) pharmalyte 3-11NL (GE Healthcare)) and 2D proteome analysis was carried out with the same conditions as previously described.

After electrophoresis run, gels were fixed (methanol 50% (v/v) acetic acid 10% (v/v)) overnight, stained with Pro-Q® Diamond phosphoprotein gel stain (Thermo fisher) for 90 minutes and destained for 30 minutes with destain solution (20% acetonitrile, 50 mM sodium acetate, pH 4.0). Gels were finally washed twice with ultrapure water and visualised using a Typhoon laser scanner (ex 555 nm / em 580 nm).

Gels were subsequently stained with SYPRO Ruby dye (Termo fisher) in order to stain all protein spots. Gels were stained on an orbital shaker overnight, then placed in wash solution (10% methanol (v/v), 7% acetic (v/v)) for 30 minutes and finally rinse twice in ultrapure water. Gels were again visualised using a Typhoon laser scanner (ex 450 nm / em 610 nm).

The ratio of Pro-Q® Diamond dye to SYPRO® Ruby dye signal intensities were calculated for each spot and this provided a measure of the phosphorylation level normalized to the total amount of protein.

Protein Identification by Mass Spectrometry (MS) and Database Searching.

In order to identify the protein spots that were found to be significantly different between EL and YO groups, mass spectrometry was performed. Briefly, 2D gels were loaded with 300 µg of proteins per strip and the electrophoretic run was carried out with the same conditions described above. After staining with Colloidal Coomassie, spots of interest were excised from the gel; spots were first destained two times with a mixture of 100 mM ammonium bicarbonate (ABC) and 50% (v/v) acetonitrile (ACN) for 45 min at 22°C and then dried using 100% ACN for 15 min. Protein spots were then reduced with 25 mM ABC containing 10 mM DTT for 1 h at 60°C and then alkylated with 55 mM iodoacetamide in 25 mM ABC for 30 min in the dark at 22°C. Gels pieces were washed twice with 25 mM ABC and finally shrunk two times with 100% ACN for 15 min and dried using 100% ACN for 10 min. After the dehydratation for 1 h at 60°C, gel pieces were incubated with 13 µl of sequencing grade modified trypsin (Promega, USA; 12.5 µg/ml in 40 mM ABC with 10% ACN, pH 8.0) overnight at 40°C (Soriano *et al.*, 2006) and extracted twice with a mixture of 50% ACN–5% formic acid (FA). Extracts were dried using a vacuum centrifuge Concentrator plus (Eppendorf).
For MS and MS/MS MALDI analysis, peptides were redissolved in 4 µl of alpha-CHCA (2,5 mg/ml in 70% ACN-0.1% TFA). 1.5 µl of each sample was spotted directly onto a dry MALDI plate (ABSciex, Foster City, CA, USA). Peptides on MALDI plate were then desalted with a cold solution of 10mM ammonium phosphate and 0.1% TFA. The analysis of samples was performed using a MALDI-TOF-TOF 4800 mass spectrometer

(ABSciex). Spectra acquisition and processing was performed using the 4000 series explorer software (ABSciex) version 3.5.28193 in positive reflectron mode at fixed laser fluency with low mass gate and delayed extraction. Peptide masses were acquired by steps of 50 spectra for the range of 900 to 4000Da. MS spectra were summed from 500 laser shots from an Nd-YAG laser operating at 355 nm and 200Hz. After filtering tryptic-, keratin- and matrix-contaminant peaks up to 15 parent ions were selected for subsequent MS/MS fragmentation according to mass range, signal intensity, signal to noise ratio, and absence of neighboring masses in the MS spectrum. MS/MS spectra were acquired in 1 kV positive mode and 1000 shots were summed by increment of 50. Database searching was carried out using Mascot 2.2 (MatrixScience, London, UK) combining MS and MS/MS interrogations on human from SwissProt databank (20 321 sequences, March 2012, www.expasy.org). Positive identification was based on a Mascot score above the significance level (i.e. <5%). The reported proteins were always those with the highest number of peptide matches. Under our identification criteria, no result was found to match to multiple members of a protein family.

MS and MS/MS ORBITRAP analyses were realized using an Ultimate 3000 Rapid Separation Liquid Chromatographic (RSLC) system (Thermo Fisher Scientific) online with a hybrid LTQ-Orbitrap-Velos mass spectrometer (Thermo Fisher Scientific). Briefly, peptides were loaded and washed on a C18 reverse phase precolumn (3 μm particle size, 100 Å pore size, 150 μm i.d., 1 cm length). The loading buffer contains 98% H2O, 2% ACN and 0.1% TFA. Peptides were then separated on a C18 reverse phase resin (2 μm particle size, 100 Å pore size, 75 μm i.d., 15 cm length) with a 4 min "effective gradient" from 100% A (0.1% FA and 100% H2O) to 50% B (80% ACN, 0.085% FA and 20% H2O).

The Linear Trap Quadrupole Orbitrap mass spectrometer acquired data throughout the elution process and operated in a data dependent scheme with full MS scans acquired with the Orbitrap, followed by up to 20 LTQ MS/MS CID spectra on the most abundant ions detected in the MS scan. Mass spectrometer settings were: full MS (AGC: $1*10^6$, resolution: $6*10^4$, m/z range 400-2000, maximum ion injection time: 500 ms); MS/MS (AGC: $5*10^3$, maximum injection time: 50 ms, minimum signal threshold: 500, isolation width: 2Da, dynamic exclusion time setting: 15 s). The fragmentation was permitted of precursor with a charge state of 2, 3, 4 and up. For database searching, all the search parameters were the same as MALDI search except the precursor mass tolerance which was set to 5 ppm and the fragment mass tolerance to 0.45 Da.

Immunoblot analysis

Some spot showing expression changes with proteomic analysis, were tested by comparative immunoblotting analysis as previously described (Brocca et al., 2012). About 20 μg of muscle samples, prepared and used for 2D electrophoresis, were loaded on Any kD precast polyacrylamide gel (Biorad product). The proteins were electrotransferred to nitrocellulose membranes at 100V for 2h and the Western blot analysis was performed. Nitrocellulose membranes were blocked in 5% milk in TBST (Tris 0.02M, NaCl 0.05 M pH 7.4-7.6, 0.1% Tween20) for 1h and then incubated in primary antibody at 4°C overnight. The membranes were probed with antibody specific to Lactate dehydrogenase (rabbit-anti LDHA, Abcam), Aldolase A (mouse-anti aldolase A, Abcam), Ubiquinol-cytochrome c reductase (mouse-anti UQCRC1, Abcam), Superoxide Dismutase 1 (rabbit-anti SOD1, Abcam), Peroxiredoxin 3 (mouse-anti PRDX3, Abcam), α-β crystallin (rabbit-anti α-β crystallin, Abcam). After several rinses in TTBS (0.1% Tween-20 in TBS), the membranes were incubated in HRP-conjugated secondary antibody, rabbit-anti-mouse (Dako) or goat-anti-rabbit (Cell Signalling) for 1h at room temperature. The protein bands were visualized by an enhanced chemiluminescence method (ECL Advance, GE Healthcare product). The content of single protein investigated was assessed by determining the brightness-area product (BAP) of the protein bands.

Carbonylated proteins

Carbonylated proteins were analysed based on the method previously reported (Brocca et al., 2010). Frozen samples from each subject group were suspended in a lysis antioxidant buffer (50 mM Tris-HCl pH7.6, 250 mM NaCl, 5 mM EDTA protease inhibitor cocktail and phosphatase inhibitor cocktail), left on ice for 20 minutes and finally centrifuged at 18000 g for 20 min at 4°C. Protein concentration was determined using the RC DC™ protein assay kit (Biorad product).

The protein carbonylation level was detected using the OxyBlotTM Kit (Millipore). Carbonyl groups in the protein side chains were derivatized to 2,4-dinitrophenylhydrazone (DNP) by reaction with 2,4-dinitrophenylhydrazine (DNPH). 10 µg of proteins for each muscle sample were denatured with SDS solution at a final concentration of 6%. The DNPH solution was added to obtain the derivation; the reaction was stopped after 15 min of incubation at room temperature. The DNP-derivatized protein samples were separated by polyacrylamide gel electrophoresis (Anykd Biorad gels) followed by Western blotting. Proteins were transferred to nitrocellulose membranes at 100V for 2h, stained with Ponceau Red (Sigma) and then scanned. The membranes were blocked in 3% bovine serum albumin (BSA) for 1 h, then incubated with rabbit anti-DNP antibody for 1h at room temperature and subsequently with a horseradish peroxidase-antibody conjugate (goat anti-rabbit IgG). The membranes were treated with chemiluminescent reagents (ECL advance as describe previously) and the positive bands emitting light were detected by short exposure to photographic films.

The oxidative status was analysed quantitatively by comparison of the signal intensity of immune-positive proteins normalized on total proteins amount loaded on gels (ponceau staining signal).

Statistical analysis

Data are expressed as the mean $\pm$ SEM. In Proteome and phosphoproteome analysis the data are expressed as ratio between the average volume of a given protein in EL group and the average volume in YO group. Significant differences between EL and YO was assessed by independent samples Student's *t*-test. A $P < 0.05$ was considered statistically significant.

Results

In vivo analyses of quadriceps mass and function

Fig. 1 shows the mean values of quadriceps volume determined by MRI, maximum voluntary torque (MVC), patellar tendon force (Ft), and patellar tendon force normalized for quadriceps volume (Ft/Qvol) of the populations of young and elderly subjects. It can be observed that quadriceps volume, MVC, and Ft were significantly lower in elderly compared to young subjects. Differences were 31% for quadriceps volume, 45% for MVC, 41% for FT. Ft/Qvol was 16% lower in elderly than in young subjects, but the difference did not reach statistical significance. Ft/Qvol can be considered analogous to in vivo specific force.

Structure and function of individual muscle fibres

For each of the 10 elderly subjects (EL) and of the 10 young subjects (YO), at least 10 single muscle fibres were dissected from vastus lateralis muscle biopsies. The analysis of cross sectional area (CSA), specific force (P_0/CSA) and unloaded shortening velocity (V_0) were performed on 120 fibres of both YO and EL. The data reported focus on the pure type 1 (YO n=37; EL 37) and type 2A (YO n=30; El=45) fibres. Hybrid fibres, either type 1-2A or 2AX, were not considered as their functional properties could be affected by the concomitant presence of more than one MHC isoform. Few fibres (2%) were pure type 2X and were not sufficient to enable a reliable comparison.

Fig 2 shows significantly lower mean values of CSA, Po/CSA and Vo of type 1 and type 2A fibres in EL subjects compared to the YO subjects. CSA was 16% lower in type 1 fibres and 15% lower in type 2A fibres in elderly subjects than in the corresponding fibre types from YO (Fig. 2A). P_0/CSA was 10% lower in type 1 fibres and 26% lower in type 2A fibres (Fig. 2B) and Vo was 25% lower in type 1 fibres and 23% in type 2A fibres of EL than in corresponding fibre types of YO (Fig. 2C).

Myosin concentration was determined in all individual muscle fibres for which CSA, P_0/CSA and V_0 are reported. The trend towards lower myosin concentration (10%) in EL subjects compared to YO did not reach statistical significance (fig. 3A). The ratio between myosin and actin content (M/A), determined by densitometry of the two proteins band, in a one dimensional SDS-PAGE gel, did not show any difference between EL and YO (fig. 3B).

Analysis of MHC isoform composition in bulk muscle samples showed significantly higher MHC-1 and significantly lower MHC-2A and MHC-2X isoforms relative content in EL compared to the YO (Fig. 3C). No significant differences were found in MLC isoform distribution (Fig. 3D).

Proteomic analysis

Proteomic maps of vastus lateralis muscle of YO and EL were obtained using 2D gel electrophoresis. In each 2D-gel more than 800 protein spots were detected and analysed for differential expression (Fig. 4B). Protein spots showing significantly different expression were subsequently identified by MALDI-Tof (Table 1) and grouped based on their functional role in the following categories: myofibrillar proteins, glycolytic enzymes, oxidative enzymes, antioxidant defence systems and other proteins. Figure 4A shows the histogram representing the volume ratios of differentially expressed proteins in EL subjects compared to YO subjects. Bars pointing to the right (positive numbers on the x axis) indicate upregulation of a protein in EL, whereas bars pointing to the left (negative numbers on the x axis) indicate downregulation.

Among myofibrillar proteins, two spots identified as actin, one spot as tropomyosin, two spots as troponin T fast were downregulated, whereas one spot identified as MLC1 slow, one spot as actin, one spot as troponin T fast and one spot of actin-α-cardiac were upregulated. Since no alterations were found in myosin/actin ratio and in 2D gel actin is resolved in several spots, the actin content was additionally investigated by a immunoblotting. This analysis showed no changes in actin levels in EL compared with the YO group (fig. 5A).

Several expression changes in metabolic enzymes were identified. In EL subjects a general up-regulation in glycolytic enzymes (except for Lactate dehydrogenase LDHA) and in oxidative enzymes was observed. In particular, we found an up-regulation of pyruvate kinase 3 isoform 2, Ubiquinol-cytochrome c reductase (UQCRC1), cytochrome b-c1, cytochrome c oxidase, dihidrolipoyl dehydrogenase and of four spots identified as aldolase A. In order to confirm the variations observed, we tested the expression of LDHA, Aldolase A and UQCRC1 by comparative immunoblotting. The results confirmed proteomic analysis (fig. 5C).

Proteomic analysis showed the greatest number of spot alterations in protein belonging to the antioxidant defence systems. Higher expression of Cu/Zn Superoxide dismutase (SOD1), carbonic anhydrase-3 (CAH III), heat shock protein B6 (HspB6), Peroxiredoxin-2, 3 and 6 (PRDX2, PRDX3, PRDX6), two spots of α-β-crystallin, gluthatione S-transferase Mu 2 and gluthatione S-transferase P (GSTP1) were found in EL compared to YO.

The significant up-regulation of SOD1, PRDX3 and α-β-crystallin observed in EL subjects was subsequently confirmed by immunoblotting analysis (Fig. 5D).

Several proteins, which could not be ascribed to a specific functional group, went through significant adaptations too. Proteasome α-sub isoform-2 and neuropolypeptide h3 was significantly up-regulated in EL subjects, whereas hemoglobin and hemoglobin sub alpha were down-regulated in EL subjects compared to YO subjects.

Phosphoproteomic analysis

Total proteins extracted from Vastus lateralis of each subject were separated by 2-DE gel and subsequently subjected to phosphoproteomic analysis. Phosphoproteins were detected by Pro-Q Diamond staining and analyzed using 2D Image Platinum software. The data showed higher phosphorylation level for the following protein spots: two spots identified as MLC-2s, one spot as actin, four spots as troponin T slow, three spots as troponin T fast, GAPDH, Aldolase A, three spots as phosphoglucomutase and two spots as myoglobin (Fig. 6A).

Interestingly, the protein spots which showed higher phosphorylation did not show any change in expression level. It should be noted that phosphorylation levels were normalised on protein content of each spot. Therefore, the higher phosphorylation levels reported are independent from protein content.

Since variations of MLC-2s phosphorylation level in EL subjects were found in 2D gels, we investigated in more detail the degree of phosphorylation of MLC isoforms in order to clarify the variations observed in shortening velocity (V_0) of single muscle fibres. The analysis was carried out in mono-dimensional gels. A significant increase was found for MLC-2s isoform only (Fig. 6C).

Oxyblot analysis

The Oxyblot analysis was performed in all samples in order to detect carbonyl groups introduced into protein structure by oxidation. We determined the oxidative level of total protein content and of myosin heavy chain (MHC) isoforms separately. A trend towards a higher total protein oxidative level in EL subjects (Fig. 7A) was found, but it did not reach statistical significance. The oxidation of MHC isoforms was significantly higher in EL subjects than in YO subjects suggesting a preferential involvement of myosin in oxidation (Fig. 7B).

Discussion

The goal of the present study was to identify underlying causes of functional impairments affecting skeletal muscle fibres of older people, without the confounding impact of sedentary living or functional impairments.

The population of elderly subjects (EL) was carefully selected based on criteria which included physically and socially active men and excluded those suffering any condition potentially causing muscle wasting (McPhee *et al.*, 2013a). The values for the physical activity questionnaire (average 8.5, while <6 is sedentary), grip strength (average was 37kg, while <30kg indicates weakness) and walking speed (average was 1.64 m/s, while <0.8 m/s indicates slowness(Cruz-Jentoft *et al.*, 2010) for the older men clearly demonstrate good physical function. The upregulation of almost all the differentially expressed proteins shown by 2D proteomic maps (Fig. 4), the unchanged myosin and actin content suggested by single muscle fibres analysis (Fig. 3A-B), and the higher relative content in MHC-1 (slow isoform) and lower relative content of MHC-2A and 2X (fast isoforms) (Fig. 3C) in whole muscle samples from EL compared to YO indicate that disuse was not a relevant phenomenon in the EL population studied. In disuse, in fact, downregulation of proteins dominates proteomic maps (Brocca *et al.*, 2012; Brocca *et al.*, 2015). Moreover, lower myosin concentration in single fibres (Borina *et al.*, 2010; Brocca *et al.*, 2015) and slow to fast shift in MHC isoforms (di Prampero & Narici, 2003; Brocca *et al.*, 2012) are observed. The results obtained from the older participants can, therefore, be considered as indicative of the ageing process, rather than being secondary to chronic diseases and lifestyle factors.

We will first discuss adaptations in proteins content, i.e.the quantitative adaptations of the older muscle proteome, and then the post-translation modifications of proteins , i.e.indicating qualitative adaptations of the muscle proteome. Finally, we will consider the potential impact of quantitative and qualitative adaptations of the muscle proteome on single muscle fibres specific force and unloaded shortening velocity.

Adaptations in protein content

Myosin heavy chain and myofibrillar proteins

No significant differences in myosin content in single fibres was observed (Fig. 3A). The latter result does not appear consistent with the lower myosin content we previously reported in muscle fibres from elderly subjects (D'Antona *et al.*, 2003). However, in the earlier work, elderly subjects were sedentary and disuse could have contributed to loss of myosin, in agreement with the impact of disuse on this parameter reported in recent human studies (Borina *et al.*, 2010; Pellegrino *et al.*, 2011a; Hvid *et al.*, 2016).

A fast to slow shift of MHC (Fig. 3C) was expected in healthy ageing based on the extensive motor unit remodelling affecting Vastus Lateralis (Song *et al.*, 2009) and possible preferential denervation of fast motor units with ageing (Powers *et al.*, 2012). The conflicting reports relating to MHC isoform distribution in previous papers, namely a shift toward slower phenotype, or toward faster phenotype, or no change in phenotype in elderly subjects (D'Antona *et al.*, 2003; Gelfi *et al.*, 2006; Raue *et al.*, 2007; Cohen *et al.*, 2009; Reich *et al.*, 2010; Konopka *et al.*, 2011), likely depend on the confounding and variable impact of disuse. Disuse is known to cause a slow to fast shift in MHC isoform distribution, the opposite of what would be expected on the basis of a preferential age induced denervation of fast motor units. The fast to slow shift is not supported by MLCs distribution that was not related to the MHCs distribution. This is consistent with previous evidences showing the coordinated expression between MHC and MLC isoforms is less strict in human muscles than in rodent muscles (Larsson and Moss, 1993, D'Antona et al 2002).

The down-regulation of tropomyosin, Troponin T fast and actin α cardiac identified with proteomic analysis is in agreement with the previous data reported by Gelfi et al. (Gelfi *et al.*, 2006). These adaptations can potentially affect single muscle fibre function, as outlined below.

Metabolic enzymes

The increase in oxidative enzymes in the old is in agreement with previous data (Gelfi *et al.*, 2006). It is generally believed that impaired oxidative metabolism is a major phenomenon of ageing *per se* (Chabi *et al.*, 2008; Porter *et al.*, 2015; Cartee *et al.*, 2016). However, contradictory results have been reported showing higher (Hart *et al.*, 2015) or unchanged (Rasmussen *et al.*, 2003) oxidative metabolism.

Glycolytic enzymes showed a contradictory trend. The effect of ageing on LDHA expression is controversial. Some reports showed an up-regulation (Riley *et al.*, 2002), whereas others found a down-regulation (Ringholm *et al.*, 2011a) of this protein. Interestingly, it has been shown that LDHA expression decreases in a wide variety of atrophic condition or catabolic states (Brocca *et al.*, 2010; Ringholm *et al.*, 2011b). Pyruvate kinase and Aldolase A represent two glycolytic enzymes playing a key role in ATP-generating reactions. Their up-regulation suggest a higher glycolytic activity.

Although a higher enzyme content is generally considered an index of higher activity, it does not unequivocally demonstrate an increase in reaction rate. In fact, to some extent, enzyme activity and enzyme content could be modulated independently (see below). Regardless, the adaptations of metabolic enzymes (Fig. 4) do not support the idea (Cartee *et al.*, 2016) that impaired metabolism is a major and necessary consequence of ageing *per se*.

Antioxidant defence systems

Reactive oxygen species (ROS) are among the intracellular signals constitutively controlling muscle phenotype and function (Jackson, 2016). It is generally accepted that reactive oxygen species (ROS) play a primary role in the ageing process, especially in those tissues in which the generation of free radicals is more pronounced, such as skeletal muscle (Fulle *et al.*, 2004). It has been suggested that a major determinant of lifespan could be the free radical-induced accumulation of damage to cellular macromolecules (Harman, 1956) and decline in mitochondria (Marzani *et al.*, 2005). However, the role of oxidative stress in the pathogenesis of ageing has been recently challenged and a debate is ongoing (Jackson, 2016).

Our data show a general up-regulation of antioxidant defence systems (Fig. 4), suggesting a reaction to cellular stress (Sandri, 2010). The antioxidant defence systems up-regulated in elderly men could be part of compensatory mechanisms against increased ROS production. The increased level of oxidation of myosin (Fig. 7) suggests that up-regulation of antioxidant defence systems could not fully prevent redox imbalance.

Muscle fibre atrophy and protein content

The present data show that muscle fibre atrophy occurs even in the active old, similar to what happens in sedentary ageing and in disuse. However, muscle atrophy in disuse and ageing is qualitatively different. Whereas in disuse, downregulation of proteins belonging to major functional groups occur, among which are the myofibrillar proteins and myosin (Pellegrino *et al.*, 2011a; Brocca *et al.*, 2012), in healthy ageing relatively few myofibrillar proteins are down-regulated (Fig. 4). Most functional groups are up-regulated (Fig. 4). The latter differences could be due to the mechanisms responsible for muscle mass loss. In disuse the imbalance between muscle protein synthesis (MPS) and breakdown (MPB), which ultimately cause muscle atrophy, is determined by both a decrease in protein synthesis and an increase in protein degradation and both phenomena are activated quickly and at relatively high levels especially in some disuse models (Pellegrino *et al.*, 2011b). In ageing, the role of an increase MPB has been questioned and the decrease in MPS is likely due to anabolic resistance which would cause continuous, but slow muscle mass loss (Atherton & Smith, 2012). Interestingly, whereas the extent of muscle fibre atrophy in human models of disuse or ageing with disuse was 21-31% (Borina *et al.*, 2010), 22-23% (Pellegrino *et al.*, 2011a) and 26-51% (D'Antona *et al.*, 2003), here we report a lower, 15-16% muscle fibre atrophy (Fig. 2).

Post-translational modifications of proteins

Phosphorylation

Global analysis of protein phosphorylation suggests higher phosphorylation of several proteins in healthy ageing (Fig. 6). Protein phosphorylation leads to changes in structural properties of substrates, but can also affect their protein-protein interaction network. These changes can have diverse biological outcomes, such as affecting protein subcellular localization (e.g., nuclear translocation or cytoplasmic retention), protein degradation and stability, as well as variations in intrinsic catalytic activity (Sakuma *et al.*, 2009).

Some myofibrillar proteins were affected by phosphorylation in elderly subjects (Fig. 6A, B). The phosphorylation of MLC-2s isoform and Troponin T (TnT), that can be phosphorylated by different protein kinases both in the isolated form and inside the whole troponin complex (Romanello *et al.*, 2010), could contribute to the adaptations observed in single muscle fibres function (Fig. 2) (see below).

Reversible protein phosphorylation is widely recognised as an essential post-translational modification (PTM) regulating metabolism. GAPDH catalyses the sixth step of glycolysis and thus serves to break down glucose for energy and carbon molecules. It has been shown that the activation of GAPDH was higher when the GAPDH phosphorylation was increased (Roberts-Wilson *et al.*, 2010). Phosphoglucomutase (PGM) is a critical regulator of cellular glucose utilization. It catalyses the conversion of glucose-1-phosphate to glucose-6-phosphate. PGM phosphorylation on Ser108 by p21-activated kinase 1 (Pak1) increase PGM catalytic activity leading to an increase of the glycolytic pathway (Robinson *et al.*, 2006). Aldolase A, found predominantly in muscle, degrades fructose 1,6 bisphosphate and is involved primarily in the catabolic pathway for glucose 6-phosphate. Aldolase has a phosphorylation site which could increase its activity. Collectively the latter results on enzyme phosphorylation and the proteomic data on enzyme content do not support the idea that ageing is necessarily associated to impaired energy metabolism (Cartee *et al.*, 2016).

Oxidation

Whereas the trend toward a higher oxidative level of total protein content did not reach statistical significance, MHC carbonylation was significantly higher in the older men. The latter results suggest that the up-regulation of antioxidant defence systems (Fig. 4) was not fully successful in counteracting protein oxidation. It is not surprising that myosin was carbonylated, whereas total proteins were not. Myosin, having a long half-life (Smith & Rennie, 1996), is more exposed to post-translational modifications. Myosin carbonylation could contribute to the adaptations observed in single muscle fibres function (Fig. 2) (see below). The unchanged oxidative level of total proteins assessed by oxyblot does not rule out the possibility that some proteins were significantly oxidized and could affect muscle fibres function. Indeed, it has been shown that the impact of oxidation on muscle proteome is complex (Baraibar *et al.*, 2013). The issue deserves further attention.

Structural and functional deterioration of muscle fibres

The loss of quadriceps mass and force *in vivo* (Fig.1) and the significant atrophy and impairment of specific force and unloaded shortening velocity of individual muscle single fibres *in vitro* (Fig.2) support the view that ageing per se alters muscle fibre structure and function independently from disuse and diseases. Indeed, the results are consistent with earlier studies on whole muscles *in vivo* (Aagaard *et al.*, 2010; McPhee *et al.*, 2013a) and on single muscle fibres in vitro (Larsson *et al.*, 1997; Frontera *et al.*, 2000; D'Antona *et al.*, 2003; Ochala *et al.*, 2007; Yu *et al.*, 2007) in which no specific attempt was made to differentiate between effects of disuse and ageing. The present results confirm that in such studies at least part of the altered skeletal muscle function could actually depend on ageing itself.

The lower CSA and specific force of individual muscle fibres can contribute to the lower muscle mass and strength observed *in vivo* (Fig. 1) (Aagaard *et al.*, 2010; McPhee *et al.*, 2013a). However, the relationship between whole muscle and individual muscle fibres structure and function is complex. Several other factors could be involved in impairment of in vivo function among which increased fat and connective tissue

content (Servais *et al.*, 2007), variations in muscle architecture and tendon compliance, neuromuscular junction integrity and excitation-contraction coupling (Narici & Maffulli, 2010).

The loss of specific force of individual muscle fibres in ageing can be due to lower number of acto-myosin interactions due to loss of myosin or to lower force generated per acto-myosin interaction due to altered myosin molecule function or acto-myosin kinetics. Specific force loss of individual muscle fibres has been accounted for by a disproportionate loss of myosin content compared to fibre CSA in both sedentary ageing (D'Antona *et al.*, 2003) and disuse (Borina *et al.*, 2010; Pellegrino *et al.*, 2011a). Here, the trend towards lower myosin content did not reach statistical significance suggesting that lower number of myosin heads available for interaction with actin does not play a major role in specific force loss. We cannot completely rule out that myosin content might have some, minor impact on specific force loss, due to the not high number of fibres per subject.

Neither altered myosin actin ratio (Fig. 3B) nor altered MLC isoform content (Fig. 3D) were observed and could account for the lower specific force of muscle fibres in EL.

Interestingly, the down-regulation of tropomyosin and troponin-t fast (Fig. 4) content could alter Ca^{2+} sensitivity of muscle fibres (Rennie & Tipton, 2000) and decrease force at submaximal levels of activation of the contractile apparatus. The latter phenomenon could affect force in vivo as muscles are not maximally activated in most motor tasks. Lower Ca^{2+} sensitivity cannot modulate specific force of skinned muscle fibres in vitro as they are activated by direct exposure to solution containing saturating Ca^{2+} concentrations. However, it cannot be ruled out that lower content in tropomyosin and troponin T might contribute to impair specific force by altering the stoichiometry of the sarcomere (Riley *et al.*, 2002).

TnT phosphorylation (Fig. 6) could be involved in single muscle fibres functional impairment in EL subjects. Phosphorylation of TnT by the α-isoform of protein kinase C results in a decrease in the maximal actomyosin ATPase activity and a decrease in its sensitivity to Ca^{2+} (Romanello & Sandri, 2010). Phosphorylation of TnT by protein kinase C ζ-isoform leads to a slight increase in the Ca^{2+} sensitivity of actomyosin ATPase and does not influence the maximal ATPase activity of actomyosin (Romanello & Sandri, 2010). It is supposed that these effects are due to decreased affinity of phosphorylated TnT for the actin-tropomyosin complex (Rommel *et al.*, 2001) or to phosphorylated TnT-induced decrease in the rate of liberation of reaction products from the active site of myosin (Rommel *et al.*, 2001). Moreover, there are evidences that TnT phosphorylation affect interactions of the thin filament with the thick filament (Sacheck *et al.*, 2007).

There is evidence that MHC oxidation alters the myosin molecule leading to a decrease in force generation (Powers *et al.*, 2005; Powers *et al.*, 2010). It has been recently suggested that myosin post-translational modifications actually occur in ageing (Li *et al.*, 2015). Mainly carbonylation, but also methylation and deamidation were suggested to alter both force and velocity of isolated myosin in in vitro motility assays (Li *et al.*, 2015). Here, we show that myosin can go through significant carbonylation in healthy ageing (Fig. 7) potentially contributing to muscle fibres specific force loss.

The significant reduction of maximum unloaded shortening velocity (V_0) in both type 1 and 2A fibres from EL subjects (Fig. 2C) is consistent with previous studies on muscle fibres (Larsson *et al.*, 1997; D'Antona *et al.*, 2003) and with studies showing lower actin sliding velocity on myosin from elderly subjects in in vitro motility assays (Hook *et al.*, 2001; D'Antona *et al.*, 2003). However, contradictory results showing no difference in unloaded shortening velocity between elderly and young male and female subjects have been reported (Trappe *et al.*, 2003). It has been argued that the discrepancy could depend on the heterogeneity among the population of subjects studied due to different exercise activity (D'Antona *et al.*, 2007). Here we suggest that impaired unloaded shortening velocity is a feature of healthy ageing, notwithstanding the normal level of physical activity (fig.2C).

Alterations in V_0 of muscle fibres could depend on several phenomena: variation in MLC isoform composition (Bottinelli *et al.*, 1994; Bottinelli & Reggiani, 2000; Bottinelli, 2001), alterations in the myosin molecule itself (Perkins *et al.*, 1997; Yamada *et al.*, 2006; Coirault *et al.*, 2007; Li *et al.*, 2015), variations in MLC phosphorylation (Diffee *et al.*, 1996; Olsson *et al.*, 2004; Greenberg *et al.*, 2009; Maffei *et al.*, 2014). In

this study, the distribution of MLC isoforms was unchanged (Fig. 3) and could not explain lower Vo. Several studies have suggested an impact of MLC2 phosphorylation on shortening velocity. Regulatory light chain phosphorylation causes disordering of the myosin head in the thick filament leading to changes in contractility and in the rate of cross-bridge attachment (Sweeney & Stull, 1990; Levine *et al.*, 1998; Szczesna *et al.*, 2002). In particular, phosphorylation-induced decreased velocity was observed in single muscle fibres and in isolated myosin in in vitro motility assay (Diffee *et al.*, 1996; Olsson *et al.*, 2004; Greenberg *et al.*, 2009; Maffei *et al.*, 2014). Here, higher MLC-2s phosphorylation level in elderly subjects (Fig. 6A, 6C) provides a potential explanation for the lower Vo. Moreover, it has been shown that an increase in myosin oxidation can determine a decrease in shortening velocity and in ATPase activity of myosin (Perkins *et al.*, 1997; Yamada *et al.*, 2006; Coirault *et al.*, 2007). The higher oxidation of MHC observed in EL subjects (Fig. 7B) could help explain V_0 variation.

Conclusions

The single muscle fibres or relatively active and healthy older men showed evidence of atrophy and impairment of specific force and unloaded shortening velocity compared with young men.

Our results also show imbalance of redox in older muscle and we suggest activation of the antioxidant defence systems is a compensatory mechanism.

The muscle proteome also showed qualitative changes, namely post-translational modifications, such as phosphorylation of several proteins and carbonylation of myosin. Myosin carbonylation suggests that up-regulation of antioxidant defence systems did not fully prevent redox imbalance.

The qualitative adaptations appeared to play a larger role than quantitative adaptations in the impairment of individual muscle fibres function. Myosin oxidation, rather than myosin content could significantly contribute to the lower force and velocity of shortening. MLC-2s phosphorylation can contribute to lower velocity of shortening. TnT phosphorylation can contribute to lower specific force, although we cannot exclude that lower tropomyosin and TnT content also play some role.

References

Aagaard P, Suetta C, Caserotti P, Magnusson SP & Kjaer M. (2010). Role of the nervous system in sarcopenia and muscle atrophy with aging: strength training as a countermeasure. *Scand J Med Sci Sports* **20,** 49-64.

Atherton PJ & Smith K. (2012). Muscle protein synthesis in response to nutrition and exercise. *J Physiol* **590,** 1049-1057.

Baraibar MA, Ladouce R & Friguet B. (2013). Proteomic quantification and identification of carbonylated proteins upon oxidative stress and during cellular aging. *J Proteomics* **92,** 63-70.

Bergstrom J. (1979). Muscle-biopsy needles. *Lancet* **1,** 153.

Borina E, Pellegrino MA, D'Antona G & Bottinelli R. (2010). Myosin and actin content of human skeletal muscle fibers following 35 days bed rest. *Scand J Med Sci Sports* **20,** 65-73.

Bottinelli R. (2001). Functional heterogeneity of mammalian single muscle fibres: do myosin isoforms tell the whole story? *Pflugers Arch* **443,** 6-17.

Bottinelli R, Betto R, Schiaffino S & Reggiani C. (1994). Unloaded shortening velocity and myosin heavy chain and alkali light chain isoform composition in rat skeletal muscle fibres. *J Physiol* **478 (Pt 2),** 341-349.

Bottinelli R, Canepari M, Pellegrino MA & Reggiani C. (1996). Force-velocity properties of human skeletal muscle fibres: myosin heavy chain isoform and temperature dependence. *J Physiol* **495 (Pt 2),** 573-586.

Bottinelli R & Reggiani C. (2000). Human skeletal muscle fibres: molecular and functional diversity. *Prog Biophys Mol Biol* **73,** 195-262.

Brocca L, Cannavino J, Coletto L, Biolo G, Sandri M, Bottinelli R & Pellegrino MA. (2012). The time course of the adaptations of human muscle proteome to bed rest and the underlying mechanisms. *J Physiol* **590,** 5211-5230.

Brocca L, Longa E, Cannavino J, Seynnes O, de Vito G, McPhee J, Narici M, Pellegrino MA & Bottinelli R. (2015). Human skeletal muscle fibre contractile properties and proteomic profile: Adaptations to 3-week unilateral lower limb suspension and active recovery. *J Physiol*.

Brocca L, Pellegrino MA, Desaphy JF, Pierno S, Camerino DC & Bottinelli R. (2010). Is oxidative stress a cause or consequence of disuse muscle atrophy in mice? A proteomic approach in hindlimb-unloaded mice. *Exp Physiol* **95,** 331-350.

Capitanio D, Vasso M, Fania C, Moriggi M, Viganò A, Procacci P, Magnaghi V & Gelfi C. (2009). Comparative proteomic profile of rat sciatic nerve and gastrocnemius muscle tissues in ageing by 2-D DIGE. *Proteomics* **9,** 2004-2020.

Cartee GD, Hepple RT, Bamman MM & Zierath JR. (2016). Exercise Promotes Healthy Aging of Skeletal Muscle. *Cell Metab* **23,** 1034-1047.

Chabi B, Ljubicic V, Menzies KJ, Huang JH, Saleem A & Hood DA. (2008). Mitochondrial function and apoptotic susceptibility in aging skeletal muscle. *Aging Cell* **7,** 2-12.

Cohen S, Brault JJ, Gygi SP, Glass DJ, Valenzuela DM, Gartner C, Latres E & Goldberg AL. (2009). During muscle atrophy, thick, but not thin, filament components are degraded by MuRF1-dependent ubiquitylation. *J Cell Biol* **185,** 1083-1095.

Coirault C, Guellich A, Barbry T, Samuel JL, Riou B & Lecarpentier Y. (2007). Oxidative stress of myosin contributes to skeletal muscle dysfunction in rats with chronic heart failure. *American journal of physiology Heart and circulatory physiology* **292,** H1009-1017.

Cruz-Jentoft AJ, Baeyens JP, Bauer JM, Boirie Y, Cederholm T, Landi F, Martin FC, Michel JP, Rolland Y, Schneider SM, Topinková E, Vandewoude M, Zamboni M & People EWGoSiO. (2010). Sarcopenia: European consensus on definition and diagnosis: Report of the European Working Group on Sarcopenia in Older People. *Age Ageing* **39,** 412-423.

D'Antona G, Lanfranconi F, Pellegrino MA, Brocca L, Adami R, Rossi R, Moro G, Miotti D, Canepari M & Bottinelli R. (2006). Skeletal muscle hypertrophy and structure and function of skeletal muscle fibres in male body builders. *J Physiol* **570,** 611-627.

D'Antona G, Pellegrino MA, Adami R, Rossi R, Carlizzi CN, Canepari M, Saltin B & Bottinelli R. (2003). The effect of ageing and immobilization on structure and function of human skeletal muscle fibres. *J Physiol* **552,** 499-511.

D'Antona G, Pellegrino MA, Carlizzi CN & Bottinelli R. (2007). Deterioration of contractile properties of muscle fibres in elderly subjects is modulated by the level of physical activity. *Eur J Appl Physiol* **100,** 603-611.

Dalla Libera L, Ravara B, Gobbo V, Danieli Betto D, Germinario E, Angelini A & Vescovo G. (2005). Skeletal muscle myofibrillar protein oxidation in heart failure and the protective effect of Carvedilol. *J Mol Cell Cardiol* **38,** 803-807.

di Prampero PE & Narici MV. (2003). Muscles in microgravity: from fibres to human motion. *J Biomech* **36,** 403-412.

Diffee GM, Patel JR, Reinach FC, Greaser ML & Moss RL. (1996). Altered kinetics of contraction in skeletal muscle fibers containing a mutant myosin regulatory light chain with reduced divalent cation binding. *Biophysical journal* **71,** 341-350.

Evans WJ & Campbell WW. (1993). Sarcopenia and age-related changes in body composition and functional capacity. *J Nutr* **123,** 465-468.

Fielding RA, Vellas B, Evans WJ, Bhasin S, Morley JE, Newman AB, Abellan van Kan G, Andrieu S, Bauer J, Breuille D, Cederholm T, Chandler J, De Meynard C, Donini L, Harris T, Kannt A, Keime Guibert F, Onder G, Papanicolaou D, Rolland Y, Rooks D, Sieber C, Souhami E, Verlaan S & Zamboni M. (2011). Sarcopenia: an undiagnosed condition in older adults. Current consensus definition: prevalence, etiology, and consequences. International working group on sarcopenia. *J Am Med Dir Assoc* **12,** 249-256.

Frontera WR, Hughes VA, Fielding RA, Fiatarone MA, Evans WJ & Roubenoff R. (2000). Aging of skeletal muscle: a 12-yr longitudinal study. *J Appl Physiol (1985)* **88,** 1321-1326.

Fulle S, Protasi F, Di Tano G, Pietrangelo T, Beltramin A, Boncompagni S, Vecchiet L & Fanò G. (2004). The contribution of reactive oxygen species to sarcopenia and muscle ageing. *Exp Gerontol* **39,** 17-24.

Gelfi C, Vigano A, Ripamonti M, Pontoglio A, Begum S, Pellegrino MA, Grassi B, Bottinelli R, Wait R & Cerretelli P. (2006). The Human Muscle Proteome in Aging. *J Proteome Res* **5,** 1344-1353.

Greenberg MJ, Mealy TR, Watt JD, Jones M, Szczesna-Cordary D & Moore JR. (2009). The molecular effects of skeletal muscle myosin regulatory light chain phosphorylation. *American journal of physiology Regulatory, integrative and comparative physiology* **297,** R265-274.

Harman D. (1956). Aging: a theory based on free radical and radiation chemistry. *J Gerontol* **11,** 298-300.

Hart CR, Layec G, Trinity JD, Liu X, Kim SE, Groot HJ, Le Fur Y, Sorensen JR, Jeong EK & Richardson RS. (2015). Evidence of Preserved Oxidative Capacity and Oxygen Delivery in the Plantar Flexor Muscles With Age. *J Gerontol A Biol Sci Med Sci* **70,** 1067-1076.

Hook P, Sriramoju V & Larsson L. (2001). Effects of aging on actin sliding speed on myosin from single skeletal muscle cells of mice, rats, and humans. *Am J Physiol Cell Physiol* **280,** C782-788.

Hvid LG, Brocca L, Ortenblad N, Suetta C, Aagaard P, Kjaer M, Bottinelli R & Pellegrino MA. (2016). Myosin content of single muscle fibers following short-term disuse and active recovery in young and old healthy men. *Experimental gerontology* **87,** 100-107.

Hvid LG, Ortenblad N, Aagaard P, Kjaer M & Suetta C. (2011). Effects of ageing on single muscle fibre contractile function following short-term immobilisation. *J Physiol* **589,** 4745-4757.

Jackson MJ. (2016). Reactive oxygen species in sarcopenia: Should we focus on excess oxidative damage or defective redox signalling? *Mol Aspects Med* **50,** 33-40.

Konopka AR, Trappe TA, Jemiolo B, Trappe SW & Harber MP. (2011). Myosin heavy chain plasticity in aging skeletal muscle with aerobic exercise training. *J Gerontol A Biol Sci Med Sci* **66,** 835-841.

Larsson L, Li X & Frontera WR. (1997). Effects of aging on shortening velocity and myosin isoform composition in single human skeletal muscle cells. *Am J Physiol* **272,** C638-649.

Levine RJ, Yang Z, Epstein ND, Fananapazir L, Stull JT & Sweeney HL. (1998). Structural and functional responses of mammalian thick filaments to alterations in myosin regulatory light chains. *Journal of structural biology* **122,** 149-161.

Li M, Ogilvie H, Ochala J, Artemenko K, Iwamoto H, Yagi N, Bergquist J & Larsson L. (2015). Aberrant post-translational modifications compromise human myosin motor function in old age. *Aging Cell* **14,** 228-235.

Maffei M, Longa E, Qaisar R, Agoni V, Desaphy JF, Conte Camerino D, Bottinelli R & Canepari M. (2014). Actin sliding velocity on pure myosin isoforms from hindlimb unloaded mice. *Acta Physiol (Oxf)*.

Marzani B, Felzani G, Bellomo RG, Vecchiet J & Marzatico F. (2005). Human muscle aging: ROS-mediated alterations in rectus abdominis and vastus lateralis muscles. *Exp Gerontol* **40,** 959-965.

McPhee JS, Hogrel JY, Maier AB, Seppet E, Seynnes OR, Sipila S, Bottinelli R, Barnouin Y, Bijlsma AY, Gapeyeva H, Maden-Wilkinson TM, Meskers CG, Paasuke M, Sillanpaa E, Stenroth L, Butler-Browne G, Narici MV & Jones DA. (2013a). Physiological and functional evaluation of healthy young and older men and women: design of the European MyoAge study. *Biogerontology* **14,** 325-337.

McPhee JS, Hogrel JY, Maier AB, Seppet E, Seynnes OR, Sipilä S, Bottinelli R, Barnouin Y, Bijlsma AY, Gapeyeva H, Maden-Wilkinson TM, Meskers CG, Pääsuke M, Sillanpää E, Stenroth L, Butler-Browne G, Narici MV & Jones DA. (2013b). Physiological and functional evaluation of healthy young and older men and women: design of the European MyoAge study. *Biogerontology* **14,** 325-337.

Narici MV & Maffulli N. (2010). Sarcopenia: characteristics, mechanisms and functional significance. *Br Med Bull* **95,** 139-159.

Ochala J, Frontera WR, Dorer DJ, Van Hoecke J & Krivickas LS. (2007). Single skeletal muscle fiber elastic and contractile characteristics in young and older men. *J Gerontol A Biol Sci Med Sci* **62,** 375-381.

Olsson MC, Patel JR, Fitzsimons DP, Walker JW & Moss RL. (2004). Basal myosin light chain phosphorylation is a determinant of Ca2+ sensitivity of force and activation dependence of the kinetics of

myocardial force development. *American journal of physiology Heart and circulatory physiology* **287,** H2712-2718.

Pellegrino MA, Canepari M, Rossi R, D'Antona G, Reggiani C & Bottinelli R. (2003). Orthologous myosin isoforms and scaling of shortening velocity with body size in mouse, rat, rabbit and human muscles. *J Physiol* **546,** 677-689.

Pellegrino MA, Desaphy JF, Brocca L, Pierno S, Camerino DC & Bottinelli R. (2011a). Redox homeostasis, oxidative stress and disuse muscle atrophy. *J Physiol* **589,** 2147-2160.

Pellegrino MA, Desaphy JF, Brocca L, Pierno S, Camerino DC & Bottinelli R. (2011b). Redox homeostasis, oxidative stress and disuse muscle atrophy. *The Journal of physiology* **589,** 2147-2160.

Perkins WJ, Han YS & Sieck GC. (1997). Skeletal muscle force and actomyosin ATPase activity reduced by nitric oxide donor. *J Appl Physiol (1985)* **83,** 1326-1332.

Porter C, Hurren NM, Cotter MV, Bhattarai N, Reidy PT, Dillon EL, Durham WJ, Tuvdendorj D, Sheffield-Moore M, Volpi E, Sidossis LS, Rasmussen BB & Børsheim E. (2015). Mitochondrial respiratory capacity and coupling control decline with age in human skeletal muscle. *Am J Physiol Endocrinol Metab* **309,** E224-232.

Powers SK, Duarte J, Kavazis AN & Talbert EE. (2010). Reactive oxygen species are signalling molecules for skeletal muscle adaptation. *Exp Physiol* **95,** 1-9.

Powers SK, Kavazis AN & DeRuisseau KC. (2005). Mechanisms of disuse muscle atrophy: role of oxidative stress. *Am J Physiol Regul Integr Comp Physiol* **288,** R337-344.

Powers SK, Smuder AJ & Judge AR. (2012). Oxidative stress and disuse muscle atrophy: cause or consequence? *Curr Opin Clin Nutr Metab Care* **15,** 240-245.

Prochniewicz E, Thompson LV & Thomas DD. (2007). Age-related decline in actomyosin structure and function. *Exp Gerontol* **42,** 931-938.

Rasmussen UF, Krustrup P, Kjaer M & Rasmussen HN. (2003). Human skeletal muscle mitochondrial metabolism in youth and senescence: no signs of functional changes in ATP formation and mitochondrial oxidative capacity. *Pflugers Arch* **446,** 270-278.

Raue U, Oellerer S & Rospert S. (2007). Association of protein biogenesis factors at the yeast ribosomal tunnel exit is affected by the translational status and nascent polypeptide sequence. *J Biol Chem* **282,** 7809-7816.

Reich KA, Chen YW, Thompson PD, Hoffman EP & Clarkson PM. (2010). Forty-eight hours of unloading and 24 h of reloading lead to changes in global gene expression patterns related to ubiquitination and oxidative stress in humans. *J Appl Physiol (1985)* **109,** 1404-1415.

Rennie MJ & Tipton KD. (2000). Protein and amino acid metabolism during and after exercise and the effects of nutrition. *Annu Rev Nutr* **20,** 457-483.

Riley DA, Bain JL, Thompson JL, Fitts RH, Widrick JJ, Trappe SW, Trappe TA & Costill DL. (2002). Thin filament diversity and physiological properties of fast and slow fiber types in astronaut leg muscles. *J Appl Physiol* **92,** 817-825.

Ringholm S, Bienso RS, Kiilerich K, Guadalupe-Grau A, Aachmann-Andersen NJ, Saltin B, Plomgaard P, Lundby C, Wojtaszewski JF, Calbet JA & Pilegaard H. (2011a). Bed rest reduces metabolic protein content and abolishes exercise-induced mRNA responses in human skeletal muscle. *Am J Physiol Endocrinol Metab* **301,** E649-658.

Ringholm S, Biensø RS, Kiilerich K, Guadalupe-Grau A, Aachmann-Andersen NJ, Saltin B, Plomgaard P, Lundby C, Wojtaszewski JF, Calbet JA & Pilegaard H. (2011b). Bed rest reduces metabolic protein content and abolishes exercise-induced mRNA responses in human skeletal muscle. *Am J Physiol Endocrinol Metab* **301,** E649-658.

Roberts-Wilson TK, Reddy RN, Bailey JL, Zheng B, Ordas R, Gooch JL & Price SR. (2010). Calcineurin signaling and PGC-1alpha expression are suppressed during muscle atrophy due to diabetes. *Biochim Biophys Acta* **1803,** 960-967.

Robinson KM, Janes MS, Pehar M, Monette JS, Ross MF, Hagen TM, Murphy MP & Beckman JS. (2006). Selective fluorescent imaging of superoxide in vivo using ethidium-based probes. *Proc Natl Acad Sci U S A* **103,** 15038-15043.

Romanello V, Guadagnin E, Gomes L, Roder I, Sandri C, Petersen Y, Milan G, Masiero E, Del Piccolo P, Foretz M, Scorrano L, Rudolf R & Sandri M. (2010). Mitochondrial fission and remodelling contributes to muscle atrophy. *EMBO J* **29,** 1774-1785.

Romanello V & Sandri M. (2010). Mitochondrial biogenesis and fragmentation as regulators of muscle protein degradation. *Curr Hypertens Rep* **12,** 433-439.

Rommel C, Bodine SC, Clarke BA, Rossman R, Nunez L, Stitt TN, Yancopoulos GD & Glass DJ. (2001). Mediation of IGF-1-induced skeletal myotube hypertrophy by PI(3)K/Akt/mTOR and PI(3)K/Akt/GSK3 pathways. *Nat Cell Biol* **3,** 1009-1013.

Sacheck JM, Hyatt JP, Raffaello A, Jagoe RT, Roy RR, Edgerton VR, Lecker SH & Goldberg AL. (2007). Rapid disuse and denervation atrophy involve transcriptional changes similar to those of muscle wasting during systemic diseases. *FASEB J* **21,** 140-155.

Sakuma K, Watanabe K, Hotta N, Koike T, Ishida K, Katayama K & Akima H. (2009). The adaptive responses in several mediators linked with hypertrophy and atrophy of skeletal muscle after lower limb unloading in humans. *Acta Physiol (Oxf)* **197,** 151-159.

Sandri M. (2010). Autophagy in health and disease. 3. Involvement of autophagy in muscle atrophy. *Am J Physiol Cell Physiol* **298,** C1291-1297.

Servais S, Letexier D, Favier R, Duchamp C & Desplanches D. (2007). Prevention of unloading-induced atrophy by vitamin E supplementation: links between oxidative stress and soleus muscle proteolysis? *Free Radic Biol Med* **42,** 627-635.

Shanely RA, Van Gammeren D, Deruisseau KC, Zergeroglu AM, McKenzie MJ, Yarasheski KE & Powers SK. (2004). Mechanical ventilation depresses protein synthesis in the rat diaphragm. *Am J Respir Crit Care Med* **170,** 994-999.

Shanely RA, Zergeroglu MA, Lennon SL, Sugiura T, Yimlamai T, Enns D, Belcastro A & Powers SK. (2002). Mechanical ventilation-induced diaphragmatic atrophy is associated with oxidative injury and increased proteolytic activity. *Am J Respir Crit Care Med* **166,** 1369-1374.

Shoepe TC, Stelzer JE, Garner DP & Widrick JJ. (2003). Functional adaptability of muscle fibers to long-term resistance exercise. *Med Sci Sports Exerc* **35,** 944-951.

Smith K & Rennie MJ. (1996). The measurement of tissue protein turnover. *Baillieres Clin Endocrinol Metab* **10,** 469-495.

Song Z, Ghochani M, McCaffery JM, Frey TG & Chan DC. (2009). Mitofusins and OPA1 mediate sequential steps in mitochondrial membrane fusion. *Mol Biol Cell* **20,** 3525-3532.

Soriano FX, Liesa M, Bach D, Chan DC, Palacin M & Zorzano A. (2006). Evidence for a mitochondrial regulatory pathway defined by peroxisome proliferator-activated receptor-gamma coactivator-1 alpha, estrogen-related receptor-alpha, and mitofusin 2. *Diabetes* **55,** 1783-1791.

Sweeney HL & Stull JT. (1990). Alteration of cross-bridge kinetics by myosin light chain phosphorylation in rabbit skeletal muscle: implications for regulation of actin-myosin interaction. *Proceedings of the National Academy of Sciences of the United States of America* **87,** 414-418.

Szczesna D, Zhao J, Jones M, Zhi G, Stull J & Potter JD. (2002). Phosphorylation of the regulatory light chains of myosin affects Ca2+ sensitivity of skeletal muscle contraction. *J Appl Physiol (1985)* **92,** 1661-1670.

Trappe S, Gallagher P, Harber M, Carrithers J, Fluckey J & Trappe T. (2003). Single muscle fibre contractile properties in young and old men and women. *J Physiol* **552,** 47-58.

Trappe S, Williamson D, Godard M, Porter D, Rowden G & Costill D. (2000). Effect of resistance training on single muscle fiber contractile function in older men. *J Appl Physiol (1985)* **89,** 143-152.

Yamada T, Mishima T, Sakamoto M, Sugiyama M, Matsunaga S & Wada M. (2006). Oxidation of myosin heavy chain and reduction in force production in hyperthyroid rat soleus. *J Appl Physiol (1985)* **100,** 1520-1526.

Yu F, Hedstrom M, Cristea A, Dalen N & Larsson L. (2007). Effects of ageing and gender on contractile properties in human skeletal muscle and single fibres. *Acta Physiol (Oxf)* **190,** 229-241.

Additional information

Competing interests

The authors declare no conflict of interest.

Authors contributions

LB, JSM, MN, MAP and RB Conception and design of the experiments; JSM, GDV Provision of study materials or patients; LB, EL, MC, OS, GDV Collection and assembly of data; LB, EL, OS, MAP, RB Data analysis and interpretation; LB, JSM, MN, MAP and RB Drafting the article or revising it critically for important intellectual content; RB Financial Support. All authors made comments on the manuscript and read and approved the final version.

Funding

Table 1

	Proteins	Abbreviations	Acces number	Estimated pI in 2D gels	Estimated MW in 2D gel (kDa)	SCORE	Function
	Myofibrillar proteins						
1	Myosin light chain 1 slow	MLC1s	P05976	5.1	27	120	Essential light chain of myosin.Does not bind calcium
2	Actin	ACTA	P68133	5.2	44	350	Skeletal actin is the major component of thin filaments. Together with the myosin form the actomyosin myofibrils that are responsible for the mechanism of muscle contraction
3	Actin	ACTA	P68133	5.1	43	385	
4	Actin	ACTA	P68133	5.1	42	265	
5	Tropomyosin alpha chain	TPM1	P09493	4.8	37	240	Plays a central role, in association with the troponin complex, in the calcium dependent regulation of vertebrate striated muscle contraction
6	Troponin T fast	TNNT3	**P45378**	4.9	39	423	Binds to tropomyosin and helps position it on actin and with the rest of the troponin complex modulates contraction of striated muscle
7	Troponin T fast	TNNT3	**P45378**	4.9	39	505	
8	Troponin T fast	TNNT3	**P45378**	6.7	39	481	
9	Actin α cardiac	ACTC	P68032	5.1	31	299	Actin is a dynamic structure that can adapt two states of flexibility. It has been suggested a key role during development
	Energy production system						
	Glycolytic enzymes						
10	Lactate dehydrogenase A	LDHA	P00338	8.1	34	597	Is involved in the first step of the pathway that synthesizes (S)-lactate from pyruvate
11	Pyruvate kinase 3 isoform 2	PKM	P14618	10	46	403	catalyzes the transfer of a phosphoryl group from phosphoenolpyruvate (PEP) to ADP, generating ATP
12	Fructose-biphosphate Aldolase A	ALDOA	P04075	9.9	36	493	Plays a key role in glycolysis and gluconeogenesis
13	Fructose-biphosphate Aldolase A	ALDOA	P04075	11.1	36	467	
14	Fructose-biphosphate Aldolase A	ALDOA	P04075	9.9	41	662	
15	Fructose-biphosphate Aldolase A	ALDOA	P04075	8.5	38	528	
	Oxidative enzymes						
16	Ubiquinol-cytochrome c reductase core I	***UQCRC1***	P31930	5.1	44	913	Is a component of the ubiquinol-cytochrome c reductase complex; it mediate the formation of the complex between cytochromes c and c1.
17	Cytochrome b-c1 complex sub2	UQCRC2	P22695	9.1	43	678	Is a component of the ubiquinol-cytochrome c reductase complex; the core protein 2 is required for the assembly of the complex
18	Cytochrome c oxidase sub 5A mit	COX5A	P20674	4.9	16	320	This is the heme A-containing chain of cytochrome c oxidase, the terminal oxidase in mitochondrial

						electron transport
19	Dihydrolipoyl dehydrogenase mit	DLDH	P09622	5.8	47	526	Is a component of the glycine cleavage system as well as of the alpha-ketoacid dehydrogenase complexes
	Antioxidant defence systems					
20	Cu/Zn Superoxide dismutase	SOD1	P00441	5.1	20	320	Catalyzes the dismutation of the superoxide (O_2^-) radical, produced as a by-product of oxygen metabolism, into either ordinary molecular oxygen (O_2) or hydrogen peroxide (H_2O_2)
21	Carbonic anhydrase III	CAH3	P07451	4.9	30	576	Catalyze the reversible hydration of carbon dioxide
22	Heat Shock Protein beta 6	HSPB6	O14558	5.0	19	450	work downstream of the other antioxidant defense systems by removing products caused by the formation of free radicals and by protecting cells against oxidative stress
23	Peroxiredoxin 2	PRDX2	P32119	5.1	24	360	Reduces peroxides with reducing equivalents provided through the thioredoxin system
24	Peroxiredoxin 3	PRDX3	P30048	5.0	27	247	Protects radical-sensitive enzymes from oxidative damage by a radical-generating system
25	Peroxiredoxin 6	PRDX6	P30041	5.0	29	471	Can reduce H2O2 and short chain organic, fatty acid, and phospholipid hydroperoxides. May play a role in the regulation of phospholipid turnover as well as in protection against oxidative injury
26	α-β-crystallin	CRYAB	P02511	5.3	23	213	Has chaperone-like activity, preventing aggregation of various proteins under a wide range of stress conditions
27	α-β-crystallin	CRYAB	P02511	4.9	22	408	
28	Glutathione-S-transferase Mu 2 isoform 1	GSTM2	P28161	5.0	28	902	Combines of reduced glutathione to a wide number of exogenous and endogenous hydrophobic electrophiles
29	Glutathione -S-transferase P	GSTP1	P09211	5.1	25	500	Combines of reduced glutathione to a wide number of exogenous and endogenous hydrophobic electrophiles
	Other proteins					
30	Proteasome α-sub isoform 2	PSMA2	P25787	5.0	34	142	Cleaves peptides with Arg, Phe, Tyr, Leu, and Glu adjacent to the leaving group at neutral or slightly basic pH
31	Hemoglobin sub beta	HBB	P68871	4.9	16	358	Involved in oxygen transport from the lung to the various peripheral tissues
32	Hemoglobin sub alpha	HBA	P69905	9.9	16	480	Involved in oxygen transport from the lung to the various peripheral tissues
33	Neuropolypeptide h3	PEBP1	P30086	8.2	21	455	Has a variety of functions in nervous tissue including the up-regulation of the production of coline acetyltransferase in cholinergic neurons

Table 2

	Proteins	Abbreviations	Acces number	Estimated pI in 2D gels	Estimated MW in 2D gel (kDa)	SCORE	Phosphorilation sites
	Myofibrillar proteins						
34	Myosin light chain 2 slow	MLC2s	P10916	4.9	20	370	11
35	Myosin light chain 2 slow	MLC2s	P10916	4.9	20	450	
36	Actin	ACTA	P68133	5.4	44	455	36
37	Troponin T slow	TNNT1	P13805	5.7	38	356	6
38	Troponin T slow	TNNT1	P13805	5.8	38	410	
39	Troponin T slow	TNNT1	P13805	6	38	340	
40	Troponin T slow	TNNT1	P13805	6.1	38	385	
41	Troponin T fast	TNNT3	P45378	7	38	225	13
42	Troponin T fast	TNNT3	P45378	7.1	38	540	
43	Troponin T fast	TNNT3	P45378	7.2	38	610	
44	Glyceraldehyde 3-P dehydr	GAPDH	P04406	9.8	38	505	46
45	Fructose-biph Aldolase A	ALDOA	P04075	10	37	420	40
46	Phosphoglucomutase	PGM1	P36871	6.5	58	445	39
47	Phosphoglucomutase	PGM1	P36871	6.7	58	254	
48	Phosphoglucomutase	PGM1	P36871	6.9	58	290	
49	Myoglobin	MB	P02144	7.8	17	310	14
50	Myoglobin	MB	P02144	8.0	17	390	

A **Quadriceps volume**

B **MVC torque**

C **Ft**

D **Ft/Qvol**
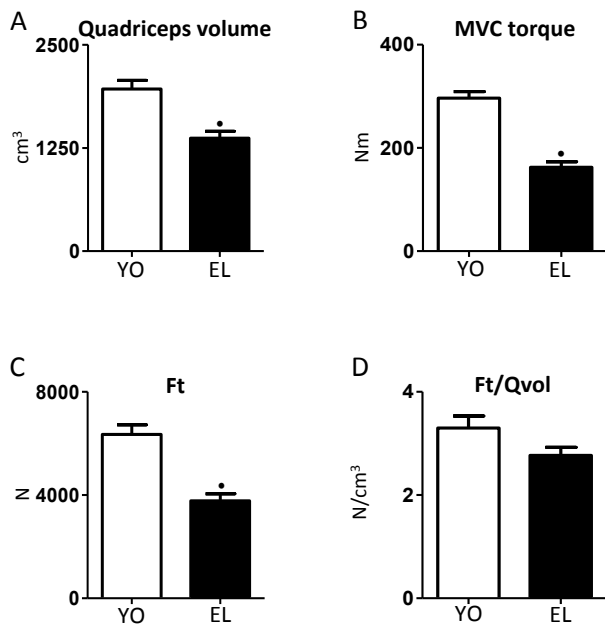
Figure 1

A

Type-1 fibres   Type-2A fibres

B

Type-1 fibres   Type-2A fibres

C

Type-1 fibres   Type-2A fibres

Figure 2

Figure 3

A

1. MLC 1 slow	
2. Actin	
3. Actin	
4. Actin	
5. Tropomyosin	Myofibrillar proteins
6. Troponin T fast	
7. Troponin T fast	
8. Troponin T fast	
9. Actin α cardiac	
10. Lactate dehydrogenase A	
11. Pyruvate kinase 3 isoform 2	
12. Fructose-biphosphate Aldolase A	Glycolytic enzymes
13. Fructose-biphosphate Aldolase A	
14. Fructose-biphosphate Aldolase A	
15. Fructose-biphosphate Aldolase A	
16. Ubiquinol-cytochrome c reductase core I	
17. Cytochrome b-c1 complex sub2	Oxidative enzymes
18. Cytochrome c oxidase sub 5A mit	
19. Dihydrolipoyl dehydrogenase mit	
20. Superoxide dismutase 1	
21. Carbonic anhydrase III	
22. Heat Shock Protein beta 6	
23. Peroxiredoxin 2	
24. Peroxiredoxin 3	Antioxidat defence systems
25. Peroxiredoxin 6	
26. α-β-crystallin	
27. α-β-crystallin	
28. Glutathione-S-transferase Mu 2 isoform 1	
29. Glutathione-S-transferase P	
30. Proteasome α-sub isoform 2	
31. Hemoglobin sub beta	Other proteins
32. Hemoglobin sub alpha	
33. Neuropolypeptide h3	

B

FIG. 4

Figure 5

A

34. MLC 2 slow	
35. MLC 2 slow	
36. Actin	
37. Troponin T slow	
38. Troponin T slow	
39. Troponin T slow	
40. Troponin T slow	
41. Troponin T fast	
42. Troponin T fast	
43. Troponin T fast	
44. Glyceraldehyde 3-P dehydr	
45. Fructose-biph Aldolase A	
46. Phosphoglucomutase	
47. Phosphoglucomutase	
48. Phosphoglucomutase	
49. myoglobin	
50. myoglobin	

B

C

MLC phosphorylation

D

Figure 6

A   Total protein oxidation

B   MHC oxidation

C

Figure 7